Provenance analysis of the Oligocene turbidites (Andaman Flysch), South Andaman Island: A geochemical approach

P C Bandopadhyay* and Biswajit Ghosh

Department of Geology, University of Calcutta, 35 Ballygunge Circular Road, Kolkata 700 019, India.
**Corresponding author. e-mail: hiyabando@yahoo.co.uk*

The Oligocene-aged sandstone-shale turbidites of the Andaman Flysch are best exposed along the east coast of the South Andaman Island. Previously undocumented sandstone-shale geochemistry, investigated here, provides important geochemical constraints on turbidite provenance. The average 70.75 wt% SiO_2, 14.52 wt% Al_2O_3, 8.2 wt% $Fe_2O_3^t$+MgO and average 0.20 Al_2O_3/SiO_2 and 1.08 K_2O/Na_2O ratios in sandstones, compare with quartzwackes. The shale samples have average 59.63 wt% SiO_2, 20.29 wt% Al_2O_3, 12.63 wt% $Fe_2O_3^t$+MgO and average 2.42 K_2O/Na_2O and 0.34 Al_2O_3/SiO_2 ratios. Geochemical data on CaO–Na_2O–K_2O diagram fall close to a granite field and on K_2O/Na_2O–SiO_2 diagram within an active continental margin tectonic setting. The range and average values of Rb and Rb/Sr ratios are consistent with acid-intermediate igneous source rocks, while the values and ratios for Cr and Ni are with mafic rocks. Combined geochemical, petrographic and palaeocurrent data indicate a dominantly plutonic-metamorphic provenance with a lesser contribution from sedimentary and volcanic source, which is possibly the Shan–Thai continental block and volcanic arc of the north-eastern and eastern Myanmar. Chemical index of alteration (CIA) values suggests a moderate range of weathering of a moderate relief terrane under warm and humid climate.

1. Introduction

Clastic sedimentary rocks, sandstones and shale in particular, contain important information about the compositions, weathering conditions and tectonic settings of the provenance and associated depositional basins. Geochemistry of sandstone and shale has been widely used to obtain this information (Crook 1974; Bhatia 1983; Taylor and McLennan 1985; Bhatia and Crook 1986; Condie *et al.* 1992; McLennan *et al.* 1993). Modern sands of known tectonic settings also exhibit systematic variations in framework mineralogy and chemical composition as a function of tectonic settings and provenance types (Maynard *et al.* 1982; Armstrong-Altrin 2009; Garzanti *et al.* 2013a).

In India, geochemical investigations and provenance analysis of sediments and sedimentary/meta-sedimentary rocks include studies from Himalaya to Great Nicobar Islands and Nicobar and Bengal Fans (Ingersoll and Suczek 1979; Garzanti and Van Haver 1988; Bhat and Ghosh 2001; Islam *et al.* 2002; Rashid 2002; Raza *et al.* 2002; Absar *et al.* 2009; Ghosh *et al.* 2012a, b; Garzanti *et al.* 2013a). Nevertheless, there has hardly been any attempt to study the geochemistry of turbidites (sandstone-shale rhythmites) from the Andaman–Nicobar convergent margin accretionary Island arc.

The present investigation submits major and trace element compositions for the sandstones, not determined earlier, reports chemical characteristics

Keywords. Andaman Flysch; geochemistry; provenance; Corbyn's Cove; South Andaman Island.

J. Earth Syst. Sci. **124**, No. 5, July 2015, pp. 1019–1037

of the Andaman Flysch turbidites and builds up geochemical constraints on source lithology, weathering conditions and tectonic setting of the provenance terrane and associated sedimentary basin that supplemented the petrographic data and regional studies. The Flysch succession is best exposed along the east coast of South Andaman Island near Corbyn's Cove (figure 1). In this study, Corbyn's Cove turbidite succession has been sampled and the geochemical results are used to interpret the provenance of these turbidite sandstones.

Sedimentary rocks of Paleogene and Neogene ages are ubiquitous and conspicuous in the Andaman–Nicobar Islands; ophiolites of Late Cretaceous age and meta-sedimentary rocks are of limited occurrences (figure 1). Shallow marine limestones, marls, calcareous sandstones, foraminiferal mudstones and reworked tuffs of Mio–Pliocene age (Archipelago Group), thick and extensive, deep sea siliciclastic turbidites of Oligocene age (Andaman Flysch) and mélange unit of shallow marine, volcaniclastic turbidite sandstones and conglomerates, reefoidal limestones, olistoliths, olistostromes, and tectonic breccias (Mithakhari Group) are major sedimentary formations (table 1). The Mithakhari Group (Karunakaran *et al.* 1968) is redefined as Mithakhari Mélange (Acharyya 1997, 2007; Bandopadhyay 2012).

Geological mapping together with petrological and paleontological studies during sixties (Chatterjee 1964, 1967; Karunakaran *et al.* 1964a, b, 1968) described the geologic setting, lithology

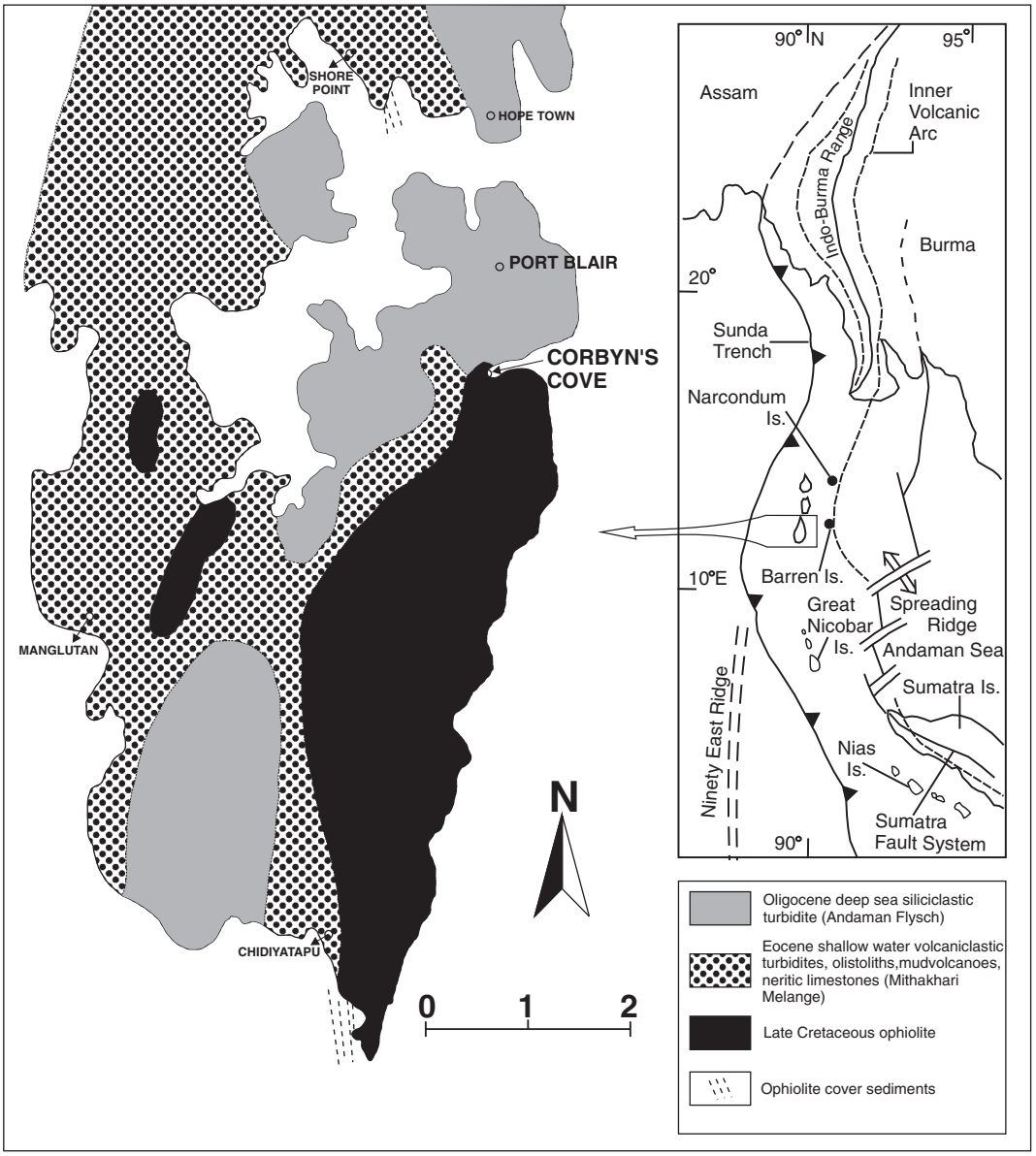

Figure 1. Outline geological map of South Andaman Island and the sample location point (Corbyn's Cove, Port Blair). Inset shows regional geotectonic setting.

Table 1. *Stratigraphy of the rocks of Andaman–Nicobar convergent margin accretionary ridge (islands) (modified after Karunakaran et al. 1968 and Bandopadhyay 2012).*

Age	Group	Formation	Structure/lithology	Sedimentary/tectonic environments/settings	Fossil record
Holocene and Pleistocene	Archipelago Group	Neil with Neil Limestone member and Chidiyatapu member (Rajashekhar and Reddy 2003)	Alluvium, mangrove, coral rags, swamp, cemented beach rock and conglomeratic shell limestone	Subaerial to intertidal	
Miocene–Pliocene	Archipelago Group	Jirkatang Limestone Muralat Chalk Melvile/ Guiter Limestone Round Chalk Strait sandstone	Cross and parallel-laminated bio-clastic limestone, marls, calcareous mudstone/siltstone, chalk, and felsic turbiditic tuffs	Shallow marine shelf	Foraminifers, *Lepidocyclina*, *Miogypsina*, *bryozoan* and algae (Sharma and Srinivasan 2007)
Oligocene (deposition between 30 and 20 Ma; Allen *et al.* 2008)		Andaman Flysch	Parallel-bedded quartzwacke-shale turbidites, Bouma sequences and sole marks are abundant.	Deep sea fan	Barren of fossil (Chatterjee 1964; Allen *et al.* 2008)
Late Paleocene–Eocene (deposition after 60 Ma and no later than 40 Ma; Allen *et al.* 2008)	Mithakhari Group (Renamed as Mithakhari Mélange (Acharyya 1997; Bandopadhyay 2012)	(3) Namunagarh Grit including Wrightmyo Nummulitic Limestone member	(3) Essentially massive and locally graded and channelized beds of gritty and coarse to medium grained volcanolithic sandstone turbidites, graded tuff, lithic-poor arkoses, and algal and foraminiferal limestones. Trace fossils and shale flake conglomerates common	(3) Shallow water basins perched on to the slopes of the accretionary wedge and fed by several small fans	*Nummulites atacicus Leymerie*, *Assilina papillata Nuttall*, *N. subatacicus Douville* and *Discocyclina* (middle Eocene); *Nummulites acutus*, *N. atacicus*, *Assilina papillata*, *Pelatispira*, *Biplanispira* (upper Eocene) (Chatterjee 1964)
		(2) Hope Town-Conglomerate with Tugapur Limestone member	(2) Matrix to clast-supported polymictic conglomerates and sandstone with shale and foraminiferal limestones	(2) Same as Namunagarh Grit	*Distichoplax biserialis* in limestones (late Paleocene) (Chatterjee 1964). *Assilina daveisi de Cizancourt* in conglomerate matrix (lower Eocene) (Chatterjee 1964)
		(1) Lipa black shale	(1) Pyritiferous black shale with olistoliths in sheared argillite matrix. Chert, muddy carbonate, mudstone, basalt, gabbro, plagiorgranite, diorite, serpentinised harzburgite, dunite, pyroxenite	(1) Euxinic environment/ trench setting. Uplifted segments of ocean floor and oceanic crust forming accretionary ridge	
Late Cretaceous to Paleocene (95 ± 1.3 Ma age of plagiogranite, Pedersen *et al.* 2010)	Ophiolite including radiolarian chert and pelagic calcareous mudstone				*Spumellarion radiolarian*, *Globigerina eugubina*, *G. trilloculinsides*, *Globorotalia compressa* and *Globotruncana* (Roy *et al.* 1988)
Pre-Ophiolite	Older metasediments		Quartz-sericite-muscovite schist, crystalline limestones, quartzite	Represent elements of passive continental margin	

and faunal content of the rocks of Andaman–Nicobar Islands and established the stratigraphy. Several subsequent studies have made significant contribution to the knowledge of geology, sedimentology, structure, stratigraphy, petrology, geochemistry, ophiolites and geodynamics (Roy 1983; Haldar 1985; Vohra *et al.* 1989; Pandey *et al.* 1992; Jafri *et al.* 1993; Acharyya 1997, 2007; Bandopadhyay and Ghosh 1998; Chakraborty *et al.* 1999; Pal *et al.* 2003; Bandopadhyay 2005, 2012; Allen *et al.* 2008; Bandopadhyay *et al.* 2008, 2009; Chakraborty and Khan 2009; Pal and Bhattacharya 2010; Pedersen *et al.* 2010; Sarma *et al.* 2010; Pal 2011; Garzanti *et al.* 2013a; Jafri and Sheikh 2013 and many others). Srinivasan and his coworkers (Sharma and Srinivasan 2007 and the references therein) have done a detailed study of the Neogene sequences of the Andaman–Nicobar Islands. In recent times, Ghosh *et al.* (2009, 2012a, b) studied the occurrences and petrology of ophiolite-associated podiform and layered chromites of Andaman Islands and discussed the petrogenetic implications of the chromite occurrences. Allen *et al.* (2008) carried out fission track (FT) and U–Pb dating of terrigeneous and volcanogenic zircon and apatite from key Paleogene sedimentary formations and provided robust and new constraints on the ages of these formations and on sedimentation-uplift history of the accretionary ridge, studying the rocks from South Andaman Island only. The Andaman–Nicobar accretionary ridge during the Oligocene collisional events between India and Asia (Acharyya 2007; Curray and Allen 2008) witnessed extensive development of deep marine siliciclastic turbidites (Andaman Flysch) for which provenance has for long, been poorly known. On the basis of palaeocurrent directions, a distal continental source beyond the northern and northeastern frontiers of Burma was broadly suggested (Karunakaran *et al.* 1964a, b, 1968; Chakraborty and Pal 2001).

2. Regional tectonic setting

The late Cretaceous–Paleogene convergence and collisional events involving subduction, off-scraping, accretion and uplift of ocean floor sediments and ophiolites along the eastern margin of the Indo-Australian plate created a north–south trending long accretionary ridge of highlands and islands that contains the Andaman–Nicobar Islands which is a non-volcanic outer arc accretionary ridge. To the north, the outer arc ridge joins the Arakan–Yoma range representing the southern prolongation of the Indo–Burma accretionary ranges (IBR) of collisional orogen. To the south, the ridge joins the outer arc islands (Nias, Banyak, Mentawai islands) of the Sumatran arc-trench system. This curvilinear belt of highlands and islands has been described as Western Sunda Arc (Curray and Allen 2008). Modern tectonic setting of the Andaman Sea region shows Andaman Sea to the east of Andaman Islands. This sea is a back arc basin above the subduction zone and regarding the origin and evolution of this basin a two-stage tectonic model has been suggested (Khan and Chakraborty 2005). A three-phase tectonic evolution since Late Oligocene for the basin has also been proposed based on the multibeam swath bathymetry, magnetic and seismological studies (Raju 2005). The volcanic islands on the Andaman Sea, Barren (active) and Narcondam (dormant) are part of the quaternary and recent inner arc volcanic belt extending from central Myanmar to Sumatra. The volcano at Barren Island since 1991 shows intermittent Strombolian eruptions (Bandopadhyay *et al.* 2014). The Andaman–Java trench lies to the west of the Andaman–Nicobar Islands (figure 1). The IBR and the Arakan–Yoma ridge in its inner or eastern part are composed primarily of Upper Cretaceous to Paleogene deep-water sediments and mélange containing blocks of gabbros, pillow basalt, serpentinite, chert, limestone and schist (Mitchell 1993). The sedimentary formations continue southward to the Andaman–Nicobar Islands where they overlie ophiolite complexes (Acharyya 1997). Farther east, the IBR is flanked by the central Myanmar (Burma) basin representing the site of continental margin between the subduction zone to the west and the arc to the east. The central Burma basin is drained by the Irrawaddy River and to the east of the basin there lies the Mogok metamorphic belt and Shan–Thai continental block of eastern Myanmar. The metamorphic belt extends for over 1500 km along the western margin of Shan plateau constituted of Precambrian to Paleozoic continental metamorphic and sedimentary rocks and intrusive igneous assemblages.

In this belt of active subduction with a strong, strike slip component, resulted from oblique convergence, off-scraped sediments and oceanic crust (ophiolite) from the subduction decollement zone has led to the formation of a subaqueous accretionary prism consisting of easterly dipping imbricate stack of thrust slices (Roy 1983; Curray 2005). Continuous underplating of the descending slab below the overriding plate beyond the margin of the trench causes up-building of the prism which with subsequent uplifts have given rise to the formation of Andaman–Nicobar subaerial ridge (islands). The ridge extends for about ∼700 km with a maximum width of ∼31 km. Olistoliths, olistostromes, slumps, slides, accretionary deformation structures, ophiolite and sedimentary mélanges, tectonic breccia, active mud diapirism, and high

seismicity, all that are characteristic of convergent margin accretionary settings, have been documented from Andaman Islands (Bandopadhyay 2012).

3. Andaman Flysch

Bounded between the Mithakhari Group below and the Archipelago Group above, the Andaman Flysch (~3000 m thick, Pal *et al.* 2003) is exposed as detached outcrops mainly along the west coast of north Andaman to south Andaman Islands. It is also exposed on the east coast of South Andaman Island from Mt. Harriet to Corbyn's Cove, where road cutting sections and wave-cut shore platforms at low tide exhibit excellent exposures of turbidites (figure 2a). The Corbyn's Cove exposures are most completely documented sequences of Andaman Flysch turbidites (Chakraborty and Pal 2001). The Flysch turbidites cover almost the entire area of Great Nicobar Island. Bandopadhyay and Ghosh (1998) and Bandopadhyay (2012) described the geologic setting and key sedimentary, petrographic and palaeontologic features of the late Paleocene–Eocene and Oligocene turbidites of the

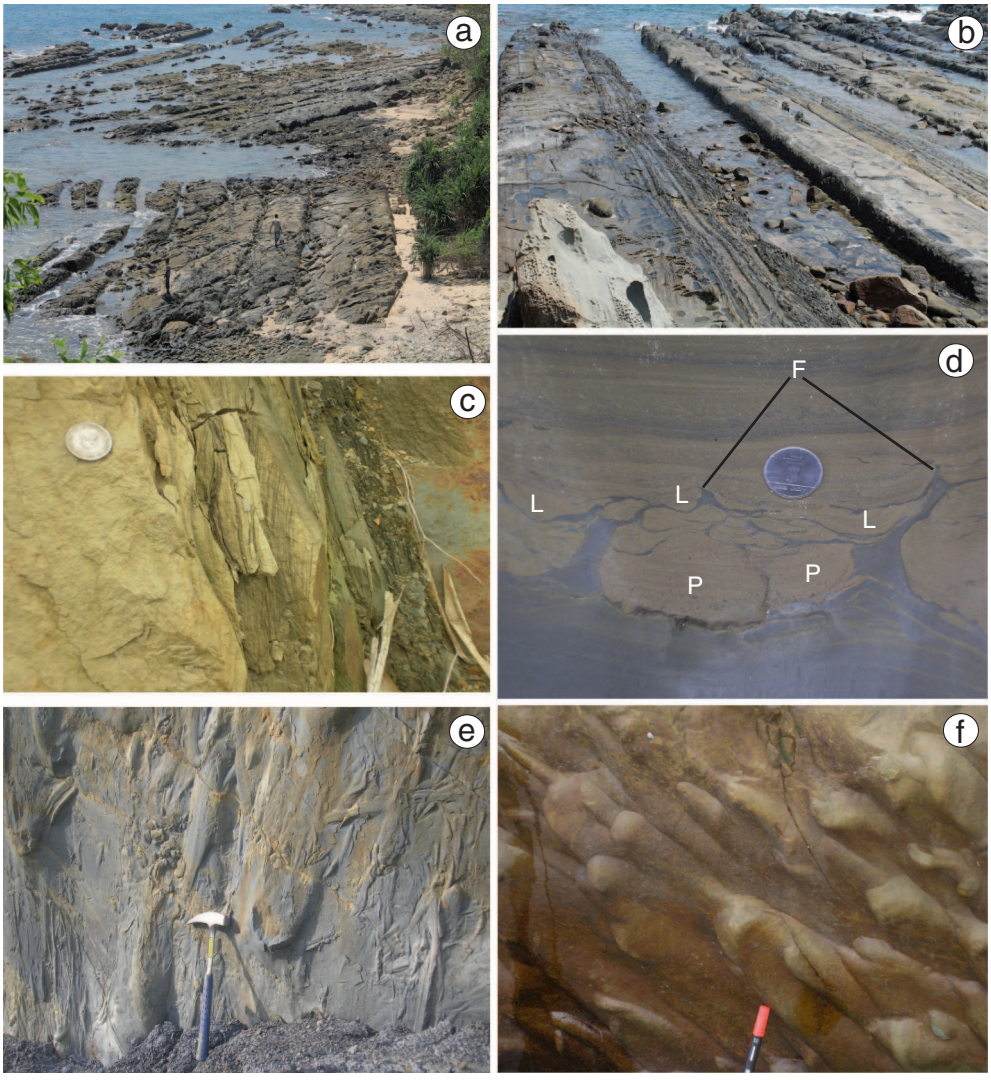

Figure 2. Field photographs of the Andaman Flysch turbidites. (**a**) Wave cut shore platform during low tide exposes faulted sequences of the meter-scale thick, steep to vertical dipping beds of turbidite sandstones interbedded with much thinner basinal shales on the east coast of South Andaman Island near Corbyn's Cove. Note the sharp change in strike of the beds due to faulting and the fault-gauge is filled with sea water, a man, 5.6 feet tall stands on a thick sandstone bed; (**b**) Meter-thick beds of sandstone showing massive lower and laminated upper part (Bouma Ta and Tb intervals) overlain by thinly laminated fissile shale; (**c**) Current ripple laminations on the top of a thick sandstone bed; (**d**) Thick sandstone bed loaded (L) into the underlying shale bed. Detached pillows (P) of sandstones within shale that intruded into the overlying sandstone bed and produce flame (F) structures; (**e**) A variety of sole marks at the base of an overturned sandstone bed, location behind airport; (**f**) A swarm of flute casts (flow direction from left to right) exposed due to overturning of the turbidite sandstone bed, South Point coastal section, Port Blair.

Andaman–Nicobar Islands and re-interpreted the age and depositional setting of the Paleogene turbidites studied earlier (Chakraborty and Pal 2001). The studied turbidites consist of meter-thick beds of light greenish grey to yellowish grey, indurated sandstones alternating with cm to dm thick beds of highly fissile and thickly-laminated dark grey shale. Individual sandstone beds are parallel-sided, up to 2-m thick and are laterally persistent, uniform in thickness, texture and composition, and show Bouma cycles. The sandstone beds with Bouma cycles, seen as most complete, start with a massive or normally graded interval at the base and grade upward to parallel laminated interval. These correspond to Bouma Ta and Tb divisions (figure 2b). A small scale current ripple-laminated interval often overlies the parallel laminated or massive interval and represents Tc division (figure 2c). However, the topmost two Bouma divisions (Td and Te) are difficult to separate in the field, and the thick and laminated beds of dark grey shale are considered as Td division. There is very little pelite division (Te) preserved. Chakraborty and Pal (2001) described top- and bottom-truncated Bouma cycles consisting of Ta-c, Tb-c, Tb-e and Td-e divisions. Individual sandstone beds are marked by a sharp base with an assemblage of sole marks (flute and groove casts and flame structures) (figure 2d–f) and a gradational top with the overlying shale. Karunakaran *et al.* (1968) and Chakraborty and Pal (2001) recorded southward palaeocurrent direction based on orientation of sole marks. They suggested sediment transport from the north and northeastern frontiers of Burma. Allen *et al.* (2008) observed that the fine to very fine grained Flysch sandstones compare closely with modern sands of homologous grain size from the Irrawaddy delta in Myanmar.

4. Sandstone petrography

4.1 *Framework minerals*

The matrix-rich, immature turbidite sandstones (figure 3a) have, for long, been described as greywackes (Karunakaran *et al.* 1964a, b and subsequent studies). Recognizing the quartzose nature of

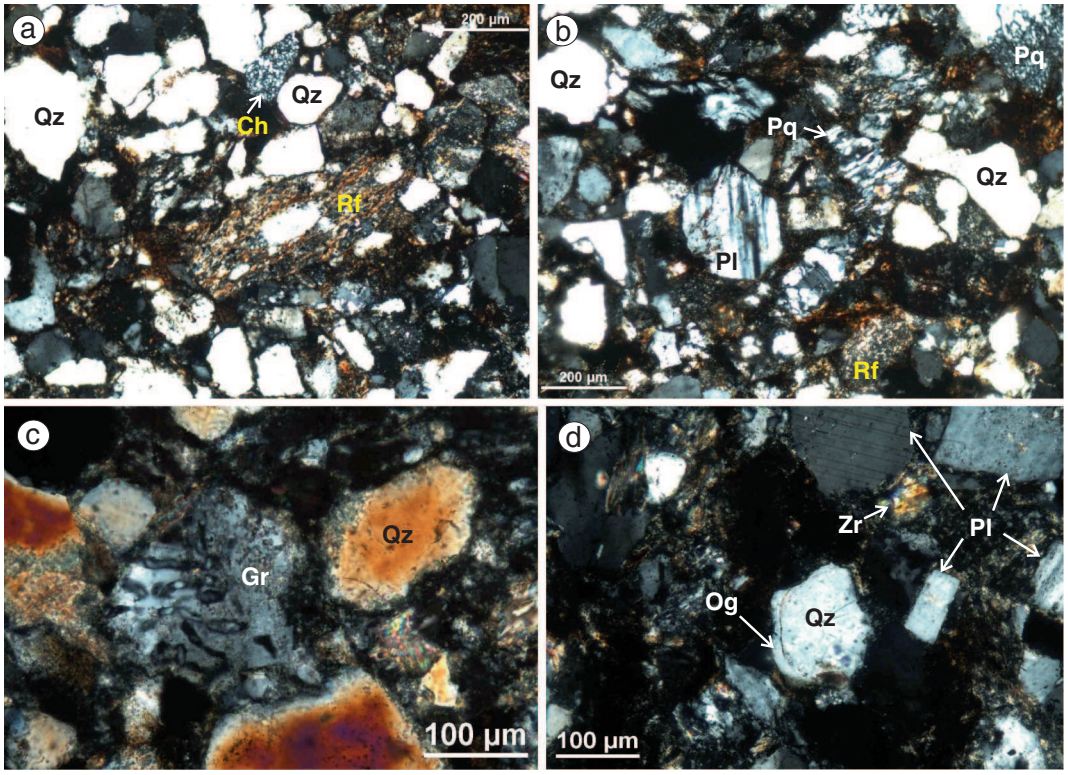

Figure 3. Photomicrographs of turbidite sandstones, Corbyn's Cove. (**a** and **b**) General view of immature quartzwacke sandstones; note schistose rock fragment (Rf), rounded chert grain (Ch) and abundance of monocrystalline quartz (Qz); (**b**) shows an almost fresh euhedral plagioclase, angular polycrystalline quartz (Pq) (middle of the photo and arrowed) consisting of numerous flattened (stretched) subgrains and strongly sutured subgrain contacts; (**c**) sand grain showing intergrowth of quartz in k-feldspar (graphic texture) and quartz grain (reddish colour) showing diffuse and corroded grain boundary; (**d**) shows abraded overgrowth of quartz (Og) on a detrital quartz grain and almost fresh untwined and twined feldspars; note a zircon grain in the middle (arrowed).

the sandstones, Bandopadhyay and Ghosh (1998) described the sandstones as quartzwackes and observed almost uniform framework compositions in different samples of the sandstones studied from Corbyn's Cove. Quartz represents the main framework components; feldspar and lithic fragments occur next in abundance. Point count analyses (Allen *et al.* 2008) indicate that the sandstones have moderate quartz (Q) content (Q: 49 ± 2%) and contain subequal amount of lithic (L) grains (L: 29 ± 6%) and feldspar (F) (F: 22 ± 6%; plagioclase feldspar 39 ± 9%). Garzanti *et al.* (2013a) provided a more actualistic nomenclature stating that the sandstones are litho-feldspatho quartzose to feldspatho-litho quartzose, metamorphiclastic with metapelites/metapsamite, rare felsic volcanics and a few sedimentary rock fragments and micas. Such petrofacies-oriented terminology provides more definite information on provenance compared to terms such as greywackes and arkoses (Ingersoll 1983). According to the classification of metamorphic rock fragments (Garzanti and Vezzoli 2003), the metamorphiclastic grains are mainly fragments of low- to medium-grade and rarely high grade metamorphic rocks (quartz-mica schist, argillites and metaquartzite) (figure 3a, b). Altered basalts and felsic volcanic grains occur in minor quantity. Sedimentaclasts include rounded grains of chert and siltstone clasts. The whole or broken, rounded sand grains, quartz with abraded overgrowth, well-rounded zircon grains, grain showing graphic texture (intergrowth of quartz in k-feldspar) and euhedral plagioclase may not be ubiquitous but are invariably conspicuous and important framework components (figure 3c and d). Among micaceous framework minerals, white muscovites followed by green-brown biotites are common. Chlorite and sericite are present in lesser amount. Micas occur as large and small flakes to very finely comminuted shreds. In places, flakes are oriented parallel to the bedding and hence to each other. Quartz grains show unit and undulose extinction but they are mostly undulose and monocrystalline variety. The common polycrystalline grains consist of a few large subgrains of unequal sizes, showing interlocking grain contacts or of several, small and flattened (stretched) subgrains showing sutured grain contacts. Feldspars comprise untwinned and chess-board twinned, k-feldspars or thin, lamellar-twinned Na-plagioclase. They are both fresh and altered; the latter looks turbid and cloudy. Zircon, tourmaline, rutile and chrome-spinel, together make up the bulk of the heavy mineral assemblages. The light pink coloured zircons comprise rounded and prismatic grains, similar to recycled and volcanic zircon respectively. Detrital framework compositions plot within recycled orogenic province of the standard QFL diagram of Dickinson *et al.* (1983) (figure 15 of Allen *et al.* 2008).

4.2 *Texture and diagenesis*

The immature turbidite sandstones show many textures and mineralogical changes resulted from moderate compaction and burial diagenetic alteration. The grain size of the studied turbidite sandstones ranges from coarse silt to medium sand but most samples are fine sand sizes. Framework quartz and feldspar grains show poor to moderate sorting but commonly very poor rounding (figure 3a, b). They are commonly angular to subangular; subrounded and rounded grains are relatively uncommon. The low sphericity framework grains are generally, moderately but locally tightly packed, showing point or long tangential grain contacts and at places, concavo–convex contacts. Diagenetically altered grains show corroded as well as diffuse grain boundaries fading gradually into the surrounding matrix (Bandopadhyay and Ghosh 1998). Diagenetically altered feldspars and muscovites show formation of illitic and kaolinitic clays and the altered biotites show formation of chlorite, along and across the cleavages and fractures. Diagenetic alteration of volcanic fragments produces chlorite, which forms along with epidote within volcanic rock fragments. Clay minerals occurring as mechanical infiltration, where observed, show thin coating around unaltered detrital grains. Alteration of framework grain produces epimatrix, while infiltration of clay minerals represents early formed protomatrix (Dickinson 1970). Micas and labile rock fragments were deformed and quashed between quartz and feldspar, and were transformed into pseudomatrix (Dickinson 1970). The framework interstices are commonly filled with dirty brown ferruginous and carbonaceous matter and fibrous clay minerals. Illite is the most common matrix mineral followed by chlorite and kaolinite. Chlorite commonly forms a pale-green fibrous aggregate. The matrix, much of which is of diagenetic origin, varies between 13 and 39 volume % of the rock and often exceeds 20%. Post-depositional alteration of minerals, particularly of mafic silicates often makes it difficult to evaluate the original clastic composition of the turbidite sandstones and in turn determination of provenance/s, source lithologies, and tectonic settings. The digenetic changes although destroy the framework mineralogy, do not affect the bulk chemical composition despite local diffusion of Na, K, Mg and Ca. The problem of diffusion of elements can be minimized in case of rapid burial. The textural and mineralogical immaturity of the sandstones and the occurrence of fresh Na-feldspars are consistent with rapid burial and concomitant reduction of effective permeability.

5. Geochemistry

5.1 *Sampling and analytical methods*

Loss of elements occur during weathering at the source region reflected in CIA values and also within sedimentation realm. Grain-size sorting during transport of sediments and mineralogical reconstitution during diagenesis, resulted in changes of chemical composition. Weathering and durability of detrital minerals in equatorial climate as in the present case, have also been investigated by Garzanti *et al.* (2013b). To minimize the effect of grain size sorting during transport and the fact that fine-grained sediments typically represent more homogeneously mixed sources (McLennan *et al.* 1993), samples of both fine-grained sandstones and the associated shale have been analyzed (cf. Roser and Korsch 1986). Diagenetic removal of elements also appears minimal because of rapid burial of the Flysch sediments (Bandopadhyay and Ghosh 1998; Allen *et al.* 2008). Eight representative samples of visibly fresh sandstone and three of interbedded shale were analyzed for major and a number of trace elements. This study based on a limited number of chemical analyses, is an initial synthesis intended to focus further study. Nevertheless, the geochemical data appear useful for an improved understanding of the petrogenesis of turbidites. Major element analyses were recalculated to 100 wt% on a volatile-free basis in order to achieve a more meaningful comparison. Major element concentrations given in wt% were determined by X-ray fluorescence spectrometric (Philips PW 1400) and the trace elements given in ppm were determined by Atomic Absorption Spectrometric (AAS) techniques. A selection of USGS standards (G2, G3, GSR-1 and BCR-1) and in-house standards were used for calibration. The analyses were performed at the chemical laboratory of the Geological Survey of India, Eastern Region. FeO and LOI were determined by wet chemistry.

5.2 *Major elements*

The range and average of concentrations of major elements and ratios of key elements for sandstone and shale of the Andaman Flysch are presented in table 2. To obtain a more realistic view, the average chemical compositions of the sandstone and shale are compared with average composition of comparable rocks of different provenances and tectonic settings (table 3). The consistent analytical results are reflected by the narrow range of variations in concentrations of major elements for both sandstone and shale. The K_2O and Na_2O contents and their ratios show a narrow range of variations and the total alkali (Na+K) content in the samples varies also within a narrow range (table 2). This could be attributed to redistribution of alkali elements during post-depositional alteration, which has not significantly affected the bulk composition. The Flysch sandstone-shale couplets show an increase of K_2O/Na_2O ratio from sandstones to shale and SiO_2 content from shale to sandstone, consistent with analysis of sandstone–mudstone suites of the greywackes, New Zealand (Roser and Korsch 1986). The CaO content in the seven samples ranges between 0.33 and 0.67 wt% (average 0.41 wt%) comparing with that of quartzwackes (Condie *et al.* 1992). The very low CaO contents reflect that the calcium resides in silicate phases and is thus considered for calculating Chemical Index of Alteration (CIA) (Nesbitt and Young 1982). One sample (no. CFHS1) with 5.99 wt% CaO shows presence of carbonate cement in petrographic thin section. All sandstone samples record extremely low MnO content (table 2), similar to that recorded by Banerjee and Banerjee (2010). The negative correlations of SiO_2 with most of the major elements in both sandstones and shale are due to most of the silica being sequestered in quartz (cf. Rahman and Suzuki 2007).

The range and average concentration of major elements of the interbedded shale (table 2) are compared with North American Shale Composite (NASC) (Gromet *et al.* 1984) and Post-Archean Average Shale (PAAS) (table 3). The NASC represents large volumes of very fine grained sediment that are thought to reflect the 'average composition' of upper continental crust; it is almost identical to the Post-Archean Average Shale (PAAS) of Taylor and McLennan (1985). The geochemistry of interbedded shales favourly compares to that of average composition of PAAS and NACS except lower CaO content compared to NACS and PAAS. When compared with mudrocks of continental arc, back arc and forearc basins (McLennan *et al.* 1990), the average composition of Flysch shale lies close to that of continental arc basin.

The chemical index of alteration (CIA; Nesbitt and Young 1982) is used to check the mobility of major elements that might have occurred, especially during diagenesis. In order to evaluate the effects of weathering, ternary diagrams that plot the molar proportions of Al_2O_3, the sum of CaO (in silicate fraction only) and Na_2O, and K_2O (A–CN–K) were constructed (Nesbitt and Young 1982). The CIA values for sandstones and shale (table 2) range between 72.70 and 85.25 (average 77.10) and for interbedded shale between 78.12 and 78.69 (average 78.46). The CIA values marginally exceed those of Phanerozoic shales (CIA = 70–75; Nesbitt and Young 1982). The current analyses of Flysch

Table 2. *Major and trace element concentrations and some key ratios for the turbidite sandstones and shale of the Andaman Flysch, Corbyn's Cove, South Andaman Island.*

	Sandstone									Shale			
Sl. no.	1	2	3	4	5	6	7	8		9	10	11	
Sample no.	CFS1	CFS2FG	CFS2YG	CFS3-11	CFS4-12	CFHS1	CF205	CF305	Avg	CFM1	CFM2	CFM3	Avg
Major element contents and their correlative ratios													
SiO_2	70.09	71	70.24	73.91	70.71	68.53	71.94	69.64	70.75	59.15	59.71	60.02	59.63
TiO_2	1.05	1.01	1.2	0.94	0.91	0.83	1.08	1.13	1.01	1.26	1.25	1.17	1.23
Al_2O_3	14.55	13.98	13.53	13.18	15.26	12.73	15.65	17.35	14.52	20.18	20.79	19.9	20.29
Fe_2O_3	3.79	3.23	3.75	3.26	3.47	2.49	5.13	7.68	4.1	5.59	3.41	5.26	4.75
FeO	2.35	2.6	2.62	2.05	1.99	2.33	0.83	0.09	1.95	3.86	5.46	4.13	4.48
MgO	2.93	3	3.4	2.3	2.47	2.42	1.83	1.19	2.44	4.22	3.28	3.76	3.75
MnO	0.06	0.06	0.06	0.04	0.05	0.33	0.04	0.02	0.08	0.1	0.07	0.15	0.11
CaO	0.67	0.64	0.63	0.33	0.49	5.99	0.06	0.06	1.12	0.46	0.43	0.44	0.44
Na_2O	2.31	2.21	2.37	1.89	2.36	1.79	1.27	0.44	1.83	1.46	1.34	1.46	1.42
K_2O	2.05	2.05	2.08	1.97	2.14	2.41	2.01	2.22	2.11	3.55	4.05	3.52	3.71
P_2O_5	0.16	0.14	0.13	0.14	0.14	0.14	0.12	0.13	0.13	0.12	0.15	0.11	0.13
Total	100.01	99.92	100.01	100.01	99.99	99.99	99.96	99.95		99.95	99.91	99.92	
LOI	3.55	3.42	3.82	3.39	3.85	7.22	1.31	5.01		8.7	8.38	7.93	
Fe_2O_3(t)	6.13	5.92	6.4	5.34	5.39	4.71	5.91	7.33	5.89	8.99	8.59	9.01	8.86
CIA	74.31	74.04	72.7	75.87	75.35	N.D.	82.41	85.25	77.1	78.67	78.12	78.59	78.46
Al_2O_3/SiO_2	0.21	0.2	0.19	0.18	0.22	0.19	0.21	0.24	0.2	0.34	0.35	0.33	0.34
SiO_2/Al_2O_3	4.81	5.07	5.19	5.6	4.63	5.38	4.59	4.01	4.91	2.93	2.87	3.02	2.94
K_2O/Na_2O	0.89	0.93	0.88	1.04	0.91	1.35	1.58	5.04	1.08	2.43	2.43	2.41	2.42
Al_2O_3/ $CaO+Na_2O$	4.88	4.9	4.51	5.94	5.35	1.64	11.74	34.02	9.12	10.51	11.18	10.47	10.72
K_2O+Na_2O	4.36	4.26	4.45	3.86	4.5	4.2	3.28	2.66	3.94	5.01	5.01	4.9	4.97
Fe_2O_3(t) + MgO	9.07	8.92	8.74	7.64	7.84	7.13	7.74	8.52	8.2	13.21	11.87	12.77	12.63
Al_2O_3/TiO_2	13.85	13.84	11.27	14.02	16.79	15.33	14.49	15.35	14.36	16.02	16.63	17	16.55

Table 2. *(Continued.)*

	Sandstone									Shale			
Sl. no.	1	2	3	4	5	6	7	8		9	10	11	
Sample no.	CFS1	CFS2FG	CFS2YG	CFS3-11	CFS4-12	CFHS1	CF205	CF305	Avg	CFM1	CFM2	CFM3	Avg
Trace element concentrations and few ratios													
Rb	45	50	50	45	40	40	68	72	51	55	85	65	68.3
Ba	275	315	250	210	210	250	400	324	279	380	430	400	403.3
Sr	125	125	130	70	105	140	67	51	101	90	95	100	95
Li	25	25	25	25	25	20	–	–		55	55	50	53.3
Cu	10	15	10	15	15	20	–	–		45	40	45	43.3
Pb	<20	<20	<20	<20	<20	<20	–	–		30	35	30	31.67
Zn	70	75	75	60	65	115	–	–	76	125	130	125	126.67
Ni	75	120	140	275	150	55	67	65	118	115	135	120	123.3
Co	20	25	25	20	20	<20	–	–		25	20	20	21.67
Cr	220	200	245	125	140	100	103	94	153	145	125	140	136.67
Zr							825	654	739				
U							5	<3					
Cr/Ni	2.93	1.66	1.75	0.45	0.93	1.81	1.53	1.44	1.29	1.26	0.93	1.17	1.12
Rb/Sr	0.36	0.4	0.38	0.64	0.38	0.28	1.01	1.41	0.61	0.58	0.89	0.65	0.71

Major element concentrations are recalculated to 100% on volatile free basis and are given in wt%. Trace elements concentrations are in ppm.

sandstones from the Wandoor outcrop, west coast of South Andaman reveal relatively higher silica content, higher K_2O/Na_2O ratio, lower Cr and Ni content, higher Rb/Sr ratios and lower CIA values, than that of the Corbyn's Cove samples with no signature of volcanic input for Wandoor samples that indicate a granite source (details will be published separately). This highlights the significant differences in compositions between Corbyn's Cove and Wandoor samples.

5.3 *Trace elements*

The range and average of eleven trace elements for sandstones and shale are presented in table 2. Cr in Flysch sandstones is in the range of 94–245 ppm (average 153 ppm), Ni 55–275 ppm (average 118 ppm) and the Cr/Ni ratios vary from 0.45 to 2.93 (average 1.29). Cr in shale is in the range of 125–145 ppm (average 136.67 ppm), Ni 115–135 ppm (average 123 ppm) and the Cr/Ni ratios vary from 0.93 to 1.17 (average 1.12). The average Cr content in Andaman Flysch compares with that of NASC and PAAS whereas average Ni content is much higher than NASC and PAAS (table 3). Among the LILE (Rb, Sr, Pb, U, Th, Ba) and HFSE (Zr, Hf, Nb, Y, Ta), concentrations of Rb, Sr, Ba and Zr are determined. The Rb content in Flysch sandstones varies from 40 to 72 ppm (average 51 ppm) and in shale from 55 to 85 ppm (average 68 ppm). The Sr in sandstones is in the range of 51–140 ppm (average 101 ppm) and in shale it is in the range of 90–100 ppm (average 95 ppm). Long *et al.* (2008) showed that the relatively high Rb concentrations (>40 ppm) and low Rb/Sr (0.04–3.24) ratio are indicative of acidic-intermediate igneous source that had undergone weak chemical weathering. In most cases, weathering and diagenetic processes can lead to a significant increase in Rb/Sr ratios and high Rb/Sr values have been interpreted as a signature of strong weathering and sedimentary recycling (McLennan *et al.* 1993). The Rb/Sr value of 16 has been interpreted as reflecting intense chemical weathering (Rashid 2002). In comparison, the average Rb/Sr values 0.61 and 0.71 in the studied sandstones and shale respectively (table 2) are lower. These ratios are higher than that of the average upper continental crust (0.32) but slightly lower than that of the average PAAS (0.80, McLennan *et al.* 1983). These comparisons reveal that the Flysch sandstones and shales have relatively low Rb/Sr ratios. Concentrations of Zr in two sandstone samples are 825 and 654 ppm (average 739 ppm). The average Zr value is higher than the average value given for average sandstone (220 ppm) (Turekian and Wedepohl 1961). This high value could be due to potential hydraulic sorting

Table 3. *Average major element compositions of sandstone (ANF) and shale (AN/C/M) of the Andaman Flysch. Sandstone composition is compared with average compositions of quartzwacke (QW) and greywacke (GW) of Alder Group (G), (Condie et al. 1992), average greywacke (Pettijohn 1987) and greywackes of Oceanic Island Arc (OIA), Continental Island Arc (CIA), Active Continental Margin (ACM), and Passive Margin (PM) (Bhatia 1983) and average composition of granite. Average composition of the interbedded shale is compared with average (A) composition of the upper continental crust (con. Crust; Taylor and McLennan 1985), North American Shale Composite (NASC) (Gromet et al. 1984) and Post-Archean Average Shale (PAAS).*

	ANF	QW (Alder G)	GW (Alder G)	AV GW	OIA GW	CIA GW	ACM GW	PM GW	AV Cont. crust	Granite	AN/C/M	PAAS	NASC
Major elements													
SiO_2	70.75	70.05	60.59	66.7	59	71	74	82	61.9	73.3	59.63	62.8	64.8
TiO_2	1.01	0.72	0.94	0.6	1.06	0.64	0.46	0.49	0.8	0.28	1.23	1	0.78
Al_2O_3	14.52	13.08	16.36	13.5	17	14	13	8	15.6	13.5	20.29	18.9	16.9
Fe_2O_3	4.1	*6.2	*8.44	1.6					2.6	2.3	4.75	6.5	5.7
FeO	1.95			3.5					3.9		4.48		
MgO	2.44	2.45	2.55	2.1					3.1	0.42	3.75	2.2	2.85
MnO	0.08										0.11	0.11	0.06
Cao	0.41	0.26	2.66	2.5	5.8	2.7	2.5	1.9	5.7	1.3	0.44	1.3	3.56
Na_2O	1.83	1.69	3.23	2.9	4.1	3.1	2.8	1.1	3.1	4.8	1.42	1.2	1.15
K_2O	2.11	3.6	2.48	2	1.1	1.9	2.9	1.7	2.9	0.08	3.71	3.7	3.99
P_2O_5	0.13	0.11	0.34								0.13	0.16	0.11
Trace elements													
Rb	51	117	88								68.3	160	125
Ba	279	678	804		370	444	522	253			403.3		636
Sr	101	114	384								95	200	142
Li	24.16										53.3		
Cu	14.17										43.3		
Pb	<20				7	15	24	16			31.67	20	
Zn	76										126.67		
Ni	118	26	56		31	13	10	8			123.3	55	58
Co	22	11	24								21.67		25.7
Cr	153	72	105		37	51	26	39			136.67	110	124.5
Zr	739	194	172		96	229	179	298				210	200
Cr/Ni	1.30	2.77	1.88		1.19	3.92	2.60	4.88			1.11	2	2.15
n	8	8	17										

and grain-size effects (Garzanti *et al.* 2013b). Similar high values of Zr in sandstones are attributed to the presence of granite-rich rocks at the source (Banerjee and Banerjee 2010).

6. Discussion

6.1 *Geochemical classification*

Condie *et al.* (1992) proposed that although greywackes and quartzwackes show compositional overlap, they can be differentiated. Quartzwackes range from 65–75 wt% SiO_2 content, whereas greywackes range from 50–70 wt%. Quartzwackes tend to be lower in CaO (<1 wt%), Na_2O (<2 wt%) and P_2O_5 (<0.1 wt%) than greywackes. When compared, the average composition of the Flysch sandstones (table 3) reflects relatively higher silica and lower MgO, Na_2O, CaO and K_2O contents than average greywackes and compared to that of quartzwacke sandstones (Condie *et al.* 1992). On the basis of quartz content, K_2O/Na_2O ratio and SiO_2 percentage, Crook (1974) classified the sandstones into quartz-rich, quartz-intermediate and quartz-poor types, stating that they represent different tectonic settings. The Flysch sandstones have intermediate quartz content, average SiO_2 (70.75 wt%) and K_2O/Na_2O ratios lower to marginally higher than 1 (average 1.08), reflecting that the sandstones are predominantly quartz-intermediate type. The quartzwacke geochemical classification of the studied sandstones is in good agreement with petrographic study.

6.2 *Source rock*

6.2.1 *Petrographic data*

In the quartzwacke sandstones of the Andaman Flysch, framework detritus are dominated by monocrystalline quartz and subordinate polycrystalline quartz. The dominance of stable monocrystalline quartz (Qm) over unstable polycrystalline quartz suggests that even though the turbidite sandstones are overall immature, they have recycled sedimentary sources. Rounded grains, quartz with abraded overgrowth and rounded zircons indicate a recycled (sedimentary) source. The polycrystalline quartz with a few (up to five) large subgrains showing interlocking grain contacts and grain with graphic texture are sourced from granite; those having more than five subgrains of unequal sizes and shapes and penetrative subgrain contacts were possibly sourced from low to medium-grade metamorphic rocks and those with numerous small and flattened (stretched) subgrains with strongly sutured grain contacts, indicate high-grade metamorphic source (Garzanti and Vezzoli 2003). Quartz-mica schists were invariably derived from medium-grade metamorphic rocks. Other components include a minor amount of weathered basalt, long and short prismatic zircon, and euhedral plagioclase, indicative of volcanic arc and ophiolite sources.

6.2.2 *Geochemical data*

The quartzwacke sandstones have silica content (range 68.53–73.91 wt% SiO_2; average 70.75 wt% SiO_2) that reflects the restricted range of SiO_2 variation and corresponds to the composition of average granite. Following Armstrong-Altrin (2009), classification of volcanic rocks by Le Bas *et al.* (1986) based on SiO_2 content, is used in this study to correlate the igneous parentage for the sandstones and a felsic source rock composition seems to be the best fit igneous parentage. Provenance lithology for these sandstones can also be depicted on a CaO–Na_2O–K_2O ternary diagram of Le Maître (1976) on which the average composition of andesite (A), dacite (D), granodiorite (Gr) and granite (G) are plotted (figure 4). Majority of the individual analyses and the average value for the sandstone in figure 4 are plotted close to average composition of granite. Two analyses showing very low (0.06 wt%) and high (5.99 wt%) CaO contents plot away from the average granite. Also plotting of data on the Al_2O_3/TiO_2 *vs.* SiO_2 diagram (Le Bas *et al.* 1986) show sandstone compositions fall in the field of felsic rock while that of shale falls in the intermediate field (figure 5). The Al_2O_3 and TiO_2 serve as excellent indicators of terrigeneous input, and are therefore relatively enriched in

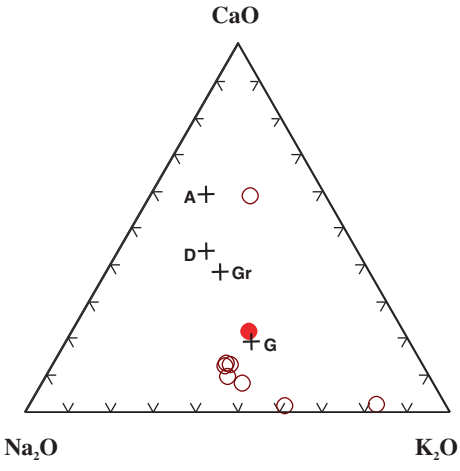

Figure 4. CaO–Na_2O–K_2O diagram showing average composition of andesite (A), dacite (D), granodiorite (Gr) and granite (G), after Le Maitre (1976). The individual (open circle) and average (solid circle) compositions of turbidite sandstones Corbyn's Cove, South Andaman Island are plotted near granite (+). Two analyses with very high and very low CaO contents plot away from the granite field. Triangle represents shale and circle represents sandstone.

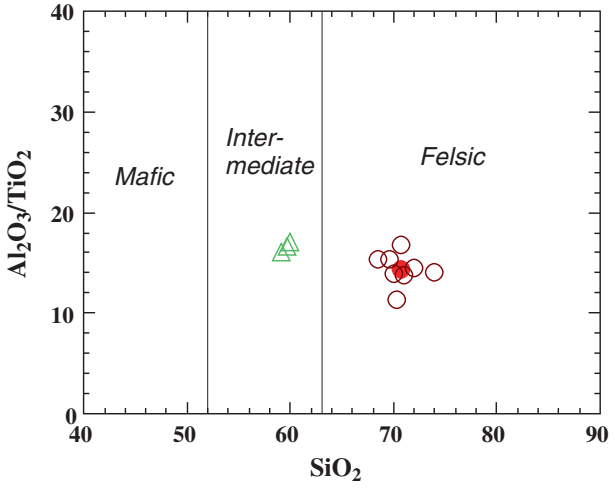

Figure 5. The Al_2O_3/TiO_2 *vs.* SiO_2 relationship for sandstone–shale turbidites. The fields are from Le Bas *et al.* (1986). Note the sandstone compositions fall in the felsic and shale in the intermediate field. Symbols are as in figure 4.

sediments deposited adjacent to, and derived from eroding continent or island arcs (Murray 1994). Statistical summary of the composition of different types of igneous rocks by Le Maitre (1976) showed that mafic rocks typically have Al_2O_3/TiO_2 values <14. Further, this ratio ranges from 3 to 8 for mafic igneous rocks, from 8 to 21 for rocks of intermediate composition and from 21 to 70 for felsic igneous rocks (Chakrabarti *et al.* 2009). The Al_2O_3/TiO_2 values in our study are in the range of 11.27–17.00 (average of 14.36) for sandstone and 16.55 (average) for shale (table 2), suggesting intermediate igneous rocks were predominant source rocks. This geochemical constraints is consistent with petrographic evidence of the dominance of quartz, alkali feldspars over plagioclase, schistose rock fragments and rarity of volcanic rock fragments. Except a slightly lower CaO and Na_2O content, the average major element composition of the interbedded shale compares with that of the upper continental crust composed of granitoid (table 3). The average composition of shale also compares to that of the shales and pelites of the Mesoproterozoic Chakrata Formation for which derivation of detritus from granite dominated upper continental crust was inferred (Rashid 2002; Raza *et al.* 2002). The Rb/Sr ratio is a measure of determining the intensity of source-rock weathering and sedimentary recycling and is also considered useful for provenance analysis (McLennan *et al.* 1993; Long *et al.* 2008). The range and average concentrations of Rb and Sr and their ratios (table 2) in sandstones and shale when compared with that of the Lower Paleozoic meta argillaceous rocks of the Chinese Altai (Long *et al.* 2008), indicate derivation of detritus from felsic-intermediate igneous source. This interpretation, based on trace element, is consistent with that inferred from the major element and the framework compositions.

On the other hand, the Cr and Ni contents and their ratios in sandstones and shale indicate presence of mafic/ultramafic rocks at the source (Hiscott 1984; Wrafter and Graham 1989; Garver *et al.* 1996). In ultramafic rocks, Cr/Ni ratio is ∼1.6 (cf. Garver *et al.* 1996). Background values of Cr and Ni in shale (NACS) are estimated to be 105 and 60 ppm respectively (Gromet *et al.* 1984). Garver *et al.* (1996) considered elevated values of Cr (>150 ppm), Ni (>100 ppm) and a Cr/Ni ratio between 1.3 and 1.5 are diagnostic of ultramafic rocks in the source region. The Cr and Ni concentrations in the studied samples are higher than the background values but are lower than the value considered indicative of ultramafic source rocks. Wrafter and Graham (1989) stated that the high Ti (>5000 ppm) and Fe (>8 wt% FeO), low Mg (∼4 to 5 wt% MgO), Cr (≡ 100 ppm) and Ni (≡< 100 ppm) indicate contribution from a mafic source whereas ultramafic source is indicated by high Mg (>8 wt% MgO) and higher Cr and Ni (>500 and >200 ppm, respectively). In comparison to these values, our data (average Cr/Ni ratio 1.29 and MgO 2.44 wt% for sandstone and average Cr/Ni ratio 1.12 and MgO 3.75 wt% for associated shale, table 2) suggest that ultramafic rocks were hardly present and the mafic rocks were present, but not widespread, at the source region. Allen *et al.* (2008) suggested a subordinate contribution from mafic volcanic rocks in the Flysch sandstones.

6.3 *Provenance terrane*

Dickinson *et al.* (1983) classified three main categories of provenance terranes. Recently Garzanti *et al.* (2007) classified five primary categories; magmatic arc, ophiolite, axial belt, continental block and clastic wedge sediment provenances that accommodate more variants of tectonic settings and clear many complexities of provenance study. Continental blocks (stable craton and uplifted basement), magmatic arcs and recycled orogens are included in Dickinson's classification. The corresponding tectonic settings are continental interior (stable craton), rift shoulder or transform rupture (uplifted basement), island arc or continental arc (magmatic arcs) and subduction complexes or fold-thrust belts (recycled orogen) respectively. Within recycled orogen, sediment sources are sedimentary, meta-sedimentary and volcano-plutonic igneous rocks exposed to erosion by orogenic uplift of fold belts and thrust sheets during continental collisional events (Dickinson *et al.* 1983). A recycled

orogenic provenance has been suggested for the quartzwacke sandstones of the Tonto Basin, Central Arizona (Condie *et al.* 1992). The studied geochemical and petrographic proxies together suggest a dual provenance consisting of a recycled orogen and a volcanic arc (continental block and magmatic arc provenances of Garzanti 2007) for the turbidites with predominant input of detritus from the recycled orogen consisting of older continental crust (McLennan *et al.* 1990). This type of source terrane as indicated by paleocurrent direction must have been located to the north and northeast of the study area. The eastern and northeastern continental region of Myanmar, where Precambrian to late Paleozoic, intermediate to felsic igneous rocks of the Shan–Thai Block and metamorphic rocks of the Mogok metamorphic belt and the associated sedimentary rocks exposed, possibly the most likely provenance. The mafic source may be the mafic volcanic rocks of arc massif that existed and extended all along the western side of the Myanmar–Malaya–Thai peninsula during late Cretaceous subduction events (Mitchell 1993). Allen *et al.* (2008) based on sandstone petrography and Sm–Nd isotope study also suggested that the source for the Flysch sandstones is likely to be the northeastern Myanmar continental region and a subordinate source is likely that of the volcanic arc in the east Myanmar.

6.4 *Tectonic setting*

The sandstone-dominated turbidites of the South Andaman Flysch represent a first-order indication of an active margin tectonic setting characterized by sand-rich turbidites (Mattern 2005). Sediment provenances and their corresponding tectonic settings have shown that the recycled orogenic provenance, suggested for the studied turbidites, corresponds to an active continental margin tectonic setting. Dickinson and Suczek (1979) and several subsequent studies used framework mineralogy to relate sandstone compositions to various tectonic settings (Garzanti *et al.* 2007). Roser and Korsch (1986) used a discrimination diagram (K_2O/Na_2O *vs.* SiO_2) to determine the tectonic setting of the sandstone–mudstone suites that shows SiO_2 content and K_2O/Na_2O values increase from volcanic arc to active continental margin to passive margin settings. Bhatia (1983) also discriminated tectonic settings of Paleozoic greywacke sandstones on the basis of major element data. These are oceanic island arc (OIA), continental island arc (CIA), active continental margin (ACM) and passive margin (PM) settings (table 3). Later studies (Armstrong-Altrin and Verma 2005; Verma and Armstrong-Altrin 2013) have questioned the usefulness of the previous tectonic discrimination diagrams and interpreted that the diagrams of Bhatia do not work reliably and the diagram of Roser and Korsch (1986) performs somewhat better with a 32–62% success rate. Examination of current literature has, however, revealed that the diagram of Roser and Korsch is used widely with success. In K_2O/Na_2O *vs.* SiO_2 diagram, both studied sandstones and shales plot in the field of active continental margin tectonic setting (figure 6). The SiO_2/Al_2O_3 ratio (average 4.91) in Flysch sandstone is similar to many ancient turbidites of active margin and continental arc tectonic settings (Maynard *et al.* 1982; McLennan *et al.* 1990). The major element compositions of the interbedded shale resemble to that of the mudstone from the Chinese Altai, inferred to have been deposited on continental arc basin (Long *et al.* 2008). Bhatia (1983) showed that the average composition of the active continental margin type sandstones is characterized by almost equal amounts of K_2O and Na_2O and the bulk composition is similar to that of the crystalline basement of the upper continental crust. Similar observations with respect to K_2O and Na_2O abundances in the studied sandstones again support an active continental margin tectonic setting. The sandstone compositions on the K_2O/Na_2O diagram of Crook (1974) (not shown) plot in the quartz-intermediate field and quartz-rich field closer to quartz-intermediate boundary, suggesting that an active continental margin is the most likely tectonic setting. The studied geochemical signatures and the regional tectonic scenario of northern and northeastern Myanmar, already discussed

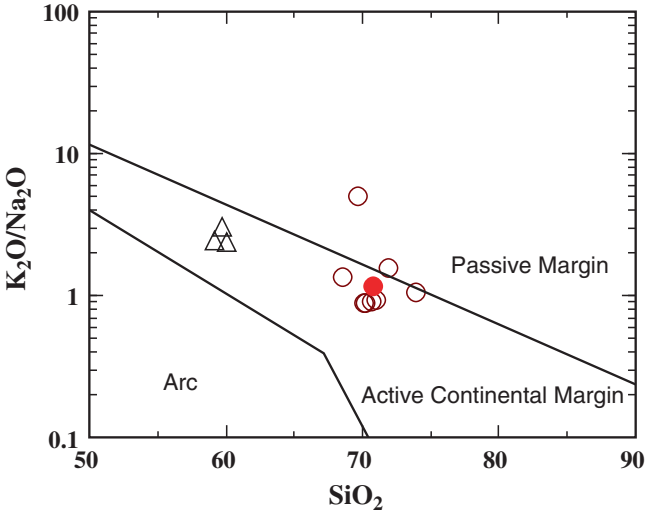

Figure 6. K_2O/Na_2O–SiO_2 diagram (after Roser and Korsch 1986) showing plots of sandstones and shales that fall in active continental margin (ACM) field including the average one (solid circle) and one close to the boundary line separating the PM and ACM field. Symbols are as in figure 4.

as active continental margin, support the above contention.

The previous studies described the Andaman Flysch as a forearc basin deposit, adjacent to the Andaman accretionary arc (Chakraborty and Pal 2001; Pal *et al.* 2003). Curray (2005) questioned that if the Flysch sandstones are forearc deposits, the source of the 3000-m thick Flysch sediments could hardly be from islands on the outer arc ridge that are very limited in size and instead, suggested that the Andaman Flysch represents, at least in part, Bengal Fan sediments. In this regard, it may also be important to note that arc-derived sands and sandstones, deposited in associated forearc/interarc basin, share characteristics of low quartz content and a high proportion of volcanic lithic grains derived from a volcano capping the arc massif (Maynard *et al.* 1982; McLennan *et al.* 1990; Tucker 2001; Garzanti *et al.* 2007). Therefore, the volcanic lithic poor, quartzose sandstones of the Andaman Flysch with a minor geochemical signature of arc input, do not suggest deposition in a forearc basin. Quartzolithic/feldspatic turbidite sandstones derived from recycled orogen, similar to those studied here, occur in Nias and Makran accretionary wedges (Moore 1979; Critelli *et al.* 1990). Critelli (1993) mentioned that the quartzose sandstones in deep marine fan are generally produced by long distance transport by the turbidity currents from a provenance in a tectonic domain not directly related to the trench. Petrofacies analysis of forearc basin turbidite sandstones, Great Valley Group, northern and central California, has shown significant presence of volcanic sands in sandstones derived from magmatic arc (Ingersoll 1983) as also observed for forearc basin sandstones in Circum-Pacific subduction complexes. Therefore, the studied Flysch turbidites which formed during the waning stage of arc volcanism, were possibly deposited as part of a submarine fan on an open ocean floor environment within an active continental margin tectonic setting associated with recycled orogenic province, before being incorporated into the outer arc of the Andaman accretionary complex. Thus, the inferred tectonic setting was not directly related to Andaman–Java trench. Bandopadhyay (2012) suggested that the Andaman Flysch was deposited beyond the influence of forearc sedimentation whereas volcanic arc signatures are very clear in rocks of the underlying volcaniclastic turbidite sandstones of the Namunagar Formation (Bandopadhyay 2005), implying significant differences in respect of their provenance. The deposition of Namunagar Formation in small fault-controlled basins within the trench-slope setting has been inferred (Karunakaran *et al.* 1968; Chakraborty *et al.* 1999).

6.5 *Paleoweathering*

The Chemical Index of Alteration (CIA) values reflect the intensity of chemical weathering in the source region (Nesbitt and Young 1982). CIA values of Phanerozoic shales generally range from 70–75, indicating moderate chemical weathering and the formation of muscovite, illite and smectite during weathering, whereas more intense weathering results in formation of kaolinite and gibbsite with CIA values approaching 100 (Nesbitt and Young 1984). Fedo *et al.* (1995) mentioned that the CIA value of 50–60 indicates an incipient weathering, 60–80 an intermediate weathering and CIA >80 extreme weathering. Values of ∼80 are generally considered as moderate weathering (Young and Nesbitt 1998). The weathering history of igneous rocks and the source for various sedimentary rocks have been examined by using A–CN–K ($A=Al_2O_3$, $CN=CaO+Na_2O$, $K=K_2O$) triangular diagram (Nesbitt and Young 1982). The diagram (figure 7) also displays the compositional trends of igneous rocks during initial stage of weathering that are almost parallel to A–CN line from their respective fresh unweathered points. CIA values for Flysch sandstones and for interbedded shale are: range 72–85 and average 77 and 78.12–78.67, average 78.46, respectively. These values are slightly higher than those of average shale estimates (CIA for pelites = 70–75). The CIA values suggest a moderate range of chemical weathering at

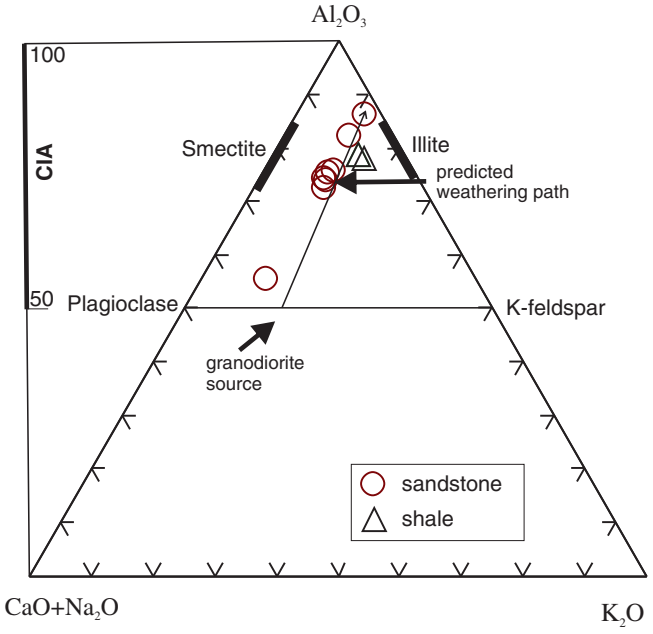

Figure 7. A–CN–K (Al_2O_3–$CaO+Na_2O$–K_2O) ternary diagram (after Nesbitt and Young 1982) showing plots of turbidite sandstones and shales cluster towards Illite field and show predicted weathering trend meets the granite–granodiorite composition. $A=Al_2O_3$, $CN=CaO+Na_2O$, $K=K_2O$, CaO= CaO in silicate phase.

the provenance and the similar values for sandstone and shale indicate the same intensity of weathering. The Rb/Sr ratio has been used to measure the intensity of weathering at the source region (Rashid 2002; Long *et al.* 2008). For the Flysch sandstone, it is 0.61 and for shale, it is 0.71 which in comparison appears low. The Rb concentration in both of them is ≥40 ppm considered to be high (Long *et al.* 2008). Therefore, the relatively high Rb concentration and low Rb/Sr ratio instead imply weak to moderate chemical weathering at the source (Long *et al.* 2008). Intensely weathered sediments show strong depletion of CaO, Na_2O and Sr (Absar *et al.* 2009). The values of CaO, Na_2O and Sr in studied turbidites, in comparison to those given by Absar *et al.* (2009) are higher and thus suggest moderate weathering. However, depletion in Al_2O_3 and enrichment in SiO_2 relative to the average composition of crust and NASC (table 3) were probably due to sedimentary sorting and loss of clays (Al_2O_3-rich, SiO_2-poor) and retention of quartz (Al_2O_3-poor, SiO_2-rich). The Al_2O_3 and TiO_2 show positive correlation in both sandstone and shale and the regression coefficient ($r = 0.57$) in comparison to strong positive correlation ($r = 0.86$; Absar *et al.* 2009) indicative of intense weathering, suggests a moderately strong correlation and in turn moderate range of weathering at the provenance. Young and Nesbitt (1998) showed that the moderate weathering is also indicated where data plots at about 70% Al_2O_3 on the Al_2O_3–(CaO+Na_2O)–K_2O triangle. We find that majority of the sandstone samples plots at about 74–75% Al_2O_3 indicating weathering at the provenance was just above the moderate range. The two sandstones and the shale samples plot at a slightly higher value indicate lower side of the intense range of weathering. Combining all these proxies, it is most likely that the Flysch sandstone was by and large subjected to moderate range of weathering.

With regard to paleoclimate and relief, it may be inferred that the sources for the sediments were exposed to climates similar to those representatives of the average Phanerozoic. The studied samples with a moderate range of CIA values cluster close to illite field in A–CN–K diagram and also plot along the granite-granodiorite weathering trend (figure 7). As the degree of weathering is a function chiefly of climate and rates of tectonic uplift (Wronkiewicz and Condie 1987), increased chemical weathering may reflect the decrease in tectonic activity and/or the change of climate towards warm and humid conditions favouring enhanced chemical weathering in the source region (Jacobson *et al.* 2003). Therefore, weathering indices of sedimentary rocks can provide useful information about the source area tectonic activity and climatic conditions. A moderate range of weathering inferred in this study, therefore indicate that the source region was a moderate relief and tectonically active terrane exposed to warm and humid paleoclimate during weathering. This is consistent with regional geology of the study area. The plots for Andaman Flysch on Al_2O_3–(CaO+Na_2O)–K_2O (ACN) ternary diagram shows that they fall away from the feldspar joining line indicating selective removal of Ca, Na and enrichment of Al_2O_3 during weathering of the source region (figure 7).

7. Conclusions

This study presents the previously undocumented major and trace element compositions of the Flysch turbidites exposed along the east coast of South Andaman and deciphers the petrogenesis of the turbidite sandstones using geochemistry reflecting quartzwacke composition of the sandstones, which received detritus from granitoid, metasedimentary and sedimentary rocks of upper continental crust and a minor amount from mafic volcanic arc, and indicates a recycled orogenic provenance. This geochemical approaches complement the information derived from petrographic study. The tectonic discrimination diagram, key element ratios and the range and average compositions of major and trace elements together with petrographic data collectively indicate that an active continental margin and associated magmatic arc appear as a best-fit tectonic settings for the provenance region of the studied Andaman Flysch. Such a provenance was likely made up of granitoid rocks with subordinate sedimentary and metamorphic rocks and arc massif. Such lithologies and palaeocurrent directions suggest that the Shan–Thai block of the northeastern Myanmar continental region as the dominant source terrane. The mafic volcanic arc of the Shan–Thai–Malaya continents also contributed detritus to the turbidites.

Acknowledgements

The paper has benefitted from the detailed and constructive criticism offered by the reviewers of the journal, who preferred to remain anonymous. Useful comments of Prof. Garzanti for the revised manuscript helped to improve the text. This research article is an outcome of a book writing project sponsored by DST, Govt. of India to PCB under USERS scheme (file no. SB/UR/14/2012). The logistic support was provided by the Department of Geology, University of Calcutta. The authors thankfully acknowledge the financial and logistic supports. Various technical helps, during

the preparation of the manuscript, received from Mr Debaditya Bandopadhyay and in subsequent stages, from Miss Sukanya Chaudhury and Miss Soumi Chatterjee, research scholars, are acknowledged with affection and appreciation.

References

Absar N, Raza M, Roy M, Naqvi S M and Roy A K 2009 Composition and weathering conditions of Paleoproterozoic upper crust of Bundelkhand craton, central India: Records from geochemistry of clastic sediments of 1.9 Ga Gwalior Group; *Precamb. Res.* **168** 313–329.

Acharyya S K 1997 Stratigraphy and tectonic history reconstruction of the Indo–Burma–Andaman mobile belt; *Indian J. Geol.* **69** 211–234.

Acharyya S K 2007 Collisional emplacement history of the Naga–Andaman ophiolites and the position of the eastern Indian suture; *J. Asian Earth Sci.* **29** 239–242.

Allen R, Carter A, Najman Y, Bandopadhyay P C, Chapman Bickle M J, Garzanti E, Vezzoli G, Andò G, Foster G L and Gerring C 2008 New constraints on the sedimentation and uplift history of the Andaman–Nicobar accretionary prism, South Andaman Island. Formation and application of sedimentary records in arc collision zone (eds) Draut A, Clift P D and Scholl D W, *Geol. Soc. Am. Spec. Publ.* **436** 223–256.

Armstrong-Altrin J S 2009 Provenance of sands from Cazones, Acapulco, and Bahia Kino beaches, Mexico; *Revista Mexicana de Ciencias Geologicas* **26** 764–782.

Armstrong-Altrin J S and Verma S P 2005 Critical evaluation of six tectonic setting discrimination diagrams using geochemical data of Neogene sediments from known tectonic settings; *Sedim. Geol.* **177** 115–129.

Bandopadhyay P C 2005 Discovery of abundant pyroclasts in Eocene Namunagarh Grit, South Andaman: Evidence for arc volcanism and subduction during the Palaeogene in the Andaman area; *J. Asian Earth Sci.* **25** 97–107.

Bandopadhyay P C 2012 Re-interpretation of the age and depositional environment of the Paleogene turbidites in Andaman and Nicobar islands, Western Sunda Arc; *J. Asian Earth Sci.* **45** 126–137.

Bandopadhyay P C and Ghosh M 1998 Facies, petrology and depositional environment of the Tertiary sedimentary rocks around Port Blair, South Andaman; *J. Geol. Soc. India* **52** 53–66.

Bandopadhyay P C, Chakrabarti U, Mohapatra N R and Roy A 2008 New field evidence of co-seismic uplift during the December 2004 earthquake, North Andaman Island; *J. Geol. Soc. India* **72** 871–874.

Bandopadhyay P C, Chakrabarti U and Roy A 2009 First report of trace fossils from Palaeogene succession (Namunagarh Grit) of Andaman and Nicobar Islands; *J. Geol. Soc. India* **73** 261–267.

Bandopadhyay P C, Ghosh B and Limonta M 2014 A reappraisal of the eruptive history and recent (1991–2009) volcanic eruptions of Barren Island, Andaman Sea; *Episode* **37** 1–14.

Banerjee A and Banerjee D M 2010 Modal analysis and geochemistry of two sandstones of the Bhander Group (late Neo-proterozoic) in parts of the central Indian Vindhyan basin and their bearing on provenance and tectonics; *J. Earth Syst. Sci.* **119** 825–839.

Bhat M I and Ghosh S K 2001 Geochemistry of 2.51 Ga old Rampur Group pelites, western Himalaya: Implications for their provenance and weathering; *Precamb. Res.* **108** 1–16.

Bhatia M R 1983 Plate tectonics and geochemical composition of sandstones; *J. Geol.* **91** 611–627.

Bhatia M R and Crook K A W 1986 Trace element characteristics of greywacke and tectonic setting discrimination of sedimentary basins; *Contrib. Mineral. Petrol.* **92** 181–193.

Chakrabarti G, Shome D, Blanca B and Sinha S 2009 Provenance and weathering history of mesoproterozoic clastic sedimentary rocks from the basal Gulcheru Formation, Cuddapah Basin; *J. Geol. Soc. India* **74** 119–130.

Chakraborty P P and Pal T 2001 Anatomy of a forearc submarine fan: Upper Eocene–Oligocene Andaman Flysch Group, Andaman Islands, India; *Gondwana Res.* **4** 477–487.

Chakraborty P P, Pal T, Duttagupta T and Gupta K S 1999 Facies pattern and depositional motif in an immature trench–slope basin, Eocene Mithakhari Group, Middle Andaman, India; *J. Geol. Soc. India* **53** 271–284.

Chakraborty P P and Khan P K 2009 Cenozoic geodynamic evolution of the Andaman–Sumatra subduction margin: Current understanding; *Island Arc.* **18** 184–200.

Chatterjee A K 1964 The Tertiary fauna of Andaman (ed.) Sunduram R K, *Int. Geol. Cong. Rept.*, 22nd Session, New Delhi, pp. 303–318.

Chatterjee P K 1967 Geology of the main islands of the Andaman; In: *Proc. Symp. Upper Mantle Project*, NGRI, Hyderabad, India, pp. 348–362.

Condie K C, Noll (Jr) P D and Conway C M 1992 Geochemical and detrital mode evidence for two sources of early Proterozoic sedimentary rocks from the Tonto basin Supergroup, central Arizona; *Sedim. Geol.* **77** 51–76.

Critelli S 1993 Sandstone detrital modes in the Paleogene Liguride complex, accretionary wedge of the southern Apennines (Italy); *J. Sedim. Petrol.* **63** 464–476.

Critelli S, De Rosa R and Platt J P 1990 Sandstone detrital mode in the Makran accretionary wedge, southwest Pakistan: Implications for tectonic setting and long distance turbidite transportation; *Sedim. Geol.* **68** 241–260.

Crook K A W 1974 Lithogenesis and geotectonics: The significance of compositional variation in flysch arenites (greywackes); *Soc. Econ. Paleontol. Mineral. Spec. Publ.* **19** 304–310.

Curray J R 2005 Tectonics and history of the Andaman Sea region; *J. Asian Earth Sci.* **25** 187–232.

Curray J R and Allen R 2008 Evolution, paleogeography and sediment provenance, Bay of Bengal, Indian Ocean; *Golden Jubilee Memoir, Geol. Soc. India* **66** 487–520.

Dickinson R W 1970 Interpreting detrital modes of greywacke and arkose; *J. Sedim. Petrol.* **40** 695–707.

Dickinson W R and Suczek C A 1979 Plate tectonics and sandstone compositions; *Am. Assoc. Petrol. Geol.* **63** 2164–2182.

Dickinson W R, Beard L S, Brakenridge G R, Erjavec J L, Ferguson R C, Inman K, Knepp R A, Lindberg F A and Ryberg P T 1983 Provenance of North American Phanerozoic sandstones in relation to tectonic setting; *Geol. Soc. Am. Bull.* **94** 222–235.

Fedo C M, Nesbitt H W and Young G M 1995 Unravelling the effects of potassium metasomatism in sedimentary rocks and paleosols, with implications for paleoweathering conditions and provenance; *Geology* **23** 921–923.

Garver J I, Royce P R and Smick T A 1996 Chromium and nickel in shale of the Taconic foreland: A case study for the provenance of fine-grained sediments with an ultramafic source; *J. Sedim. Res.* **66** 100–106.

Garzanti E and Van Haver T 1988 The Indus clastics: Forearc basin sedimentation in the Ladakh Himalaya (India); *Sedim. Geol.* **59** 237–249.

Garzanti E and Vezzoli G 2003 A classification of metamorphic grains in sands based on their composition and grade; *J. Sedim. Res.* **73** 830–837.

Garzanti E, Doglioni C, Vezzoli G and Ando S 2007 Orogenic belts and orogenic sediment provenance; *J. Geol.* **115** 315–334.

Garzanti E, Limonta M, Resentini A, Bandopadhyay P C, Najman Y, Ando S and Vezzoli V 2013a Sediment recycling at convergent plate margins: Indo-Burman Ranges and Andaman–Nicobar Ridge; *Earth Sci. Rev.* **123** 113–132.

Garzanti E, Padoan M, Ando S, Resentini A, Vezzoli G and Lustrino M 2013b Weathering and relative durability of detrital minerals in equatorial climate: Sand petrology in the East African rift; *J. Geol.* **121** 547–580.

Ghosh B, Pal T, Bhattacharya A and Das D 2009 Petrogenetic implications of ophiolitic chromite from Rutland Island, Andaman – a boninitic parentage in supra-subduction setting; *Mineral. Petrol.* **96** 59–70.

Ghosh S, Sarkar S and Ghosh P 2012a Petrography and major element geochemistry of the Permo–Triassic sandstones, central India: Implications for provenance in an intracratonic pull-apart basin; *J. Asian Earth Sci.* **43** 207–240.

Ghosh B, Morishita T and Bhatta K 2012b Detrital chromian spinels from beach placers of Andaman Islands, India: A perspective view of petrological characteristics and variations of the Andaman ophiolite; *Island Arc.* **21** 188–201.

Gromet L P, Dymek R F, Haskin L A and Korotev R L 1984 The North American shale composite: Its implications, major and trace elements characteristics; *Geochim. Cosmochim. Acta* **48** 2469–2482.

Haldar D 1985 Some aspects of Andaman ophiolite complex; *Rec. Geol. Surv. India* **115** 1–11.

Hiscott R N 1984 Ophiolitic source rocks for Taconic-age flysch: Trace element evidence; *Geol. Soc. Am. Bull.* **95** 1261–1267.

Ingersoll R V 1983 Petrofacies and provenance of late Mesozoic forearc basin, northern and central California; *Bull. Am. Assoc. Petrol. Geol.* **67** 1125–1142.

Ingersoll R V and Suczek C A 1979 Petrology and provenance of Neogene sand from Nicobar and Bengal fans, DSDP sties 211 and 218; *J. Sedim. Petrol.* **49** 1217–1228.

Islam R, Ghosh S K and Sachan H K 2002 Geochemical characterization of the Neoproterozoic Nagthat siliciclastics, NW Kumaun Lesser Himalaya: Implications for source rock assessment; *J. Geol. Soc. India* **60** 91–105.

Jacobson A D, Blum J D, Chamberlian C P, Craw D and Koons P O 2003 Climate and tectonic controls on chemical weathering in the New Zealand Southern Alps; *Geochim. Cosmochim. Acta* **37** 29–46.

Jafri S H and Sheikh J M 2013 Geochemistry of pillow basalts from Bompoka, Andaman–Nicobar Islands, Bay of Bengal, India; *J. Asian Earth Sci.* **64** 27–37.

Jafri S H, Balaram V and Govil P K 1993 Depositional environments of Cretaceous radiolarian cherts from Andaman–Nicobar Islands, northeastern Indian Ocean; *Mar. Geol.* **112** 291–301.

Karunakaran C, Pawde M B, Raina V K and Ray K K 1964a Geology of the South Andaman Island, India; Reports of the 22nd Int. Geol. Cong., New Delhi, India, XI. 79–100.

Karunakaran C, Ray K K and Saha S S 1964b Sedimentary environment of the formation of Andaman Flysch, Andaman Islands, India; Reports of the 22nd Int. Geol. Cong., New Delhi, India, XV. 226–232.

Karunakaran C, Ray K K and Saha S S 1968 Tertiary sedimentation in Andaman–Nicobar geosynclines; *J. Geol. Soc. India* **9** 32–39.

Khan P K and Chakraborty P P 2005 Two-phase opening of Andaman Sea: A new seismotectonic insight; *Earth Planet. Sci. Lett.* **229** 259–71.

Le Bas M J, Le Maitre R W, Streckeisen A and Zanettinal B 1986 A chemical classification of volcanic rocks based on the total alkali–silica diagram; *J. Petrol.* **27** 745–750.

Le Maitre R W 1976 The chemical variability of some common igneous rocks; *J. Petrol.* **17** 589–637.

Long X, Sun M, Yuan C, Xiao W and CAI K 2008 Early Paleozoic sedimentary record of the Chinese Altai: Implications for its tectonic evolution; *Sedim. Geol.* **208** 88–100.

Mattern F 2005 Ancient sand-rich submarine fans: Depositional systems, models, identification, and analysis; *Earth Sci. Rev.* **70** 167–202.

Maynard J B, Valloni R and Yu H S 1982 Composition of modern deep-sea sands from arc-related basins. Trench-forearc geology: Sedimentation and tectonics on modern and ancient active plate margins (ed.) Legget J K, *Geol. Soc. Am. Spec. Paper* **284** 21–40.

McLennan S M, Taylor S R and Eriksson K A 1983 Geochemistry of Archean shales from the Pilbara Supergroup, western Australia; *Geochim. Cosmochim. Acta* **47** 1211–1222.

McLennan S M, Taylor S R, McCulloch M T and Maynard J B 1990 Geochemical and Nd–Sr isotope composition of deep-sea turbidites: Crustal evolution and plate tectonic associations; *Geochim. Cosmochim. Acta* **54** 2015–2050.

McLennan S M, Hemming S, McDaniel D K and Hanson G N 1993 Geochemical approaches to sedimentation, provenance, and tectonics; In: Processes controlling the composition of clastic sediments (eds) Johnson M J and Basu A, *Geol. Soc. Am. Spec. Paper* **284** 21–40.

Mitchell A H G 1993 Cretaceous–Cenozoic tectonic events in the western Myanmar (Burma)–Assam region; *J. Geol. Soc. London* **150** 1089–1102.

Moore G F 1979 Petrography of subduction zone sandstones from Nias Island, Indonesia; *J. Sedim. Petrol.* **49** 71–84.

Nesbitt H W and Young G M 1982 Early Proterozoic climates and plate motions inferred from major element chemistry of lutites; *Nature* **299** 715–717.

Nesbitt H W and Young G M 1984 Prediction of some weathering trends of plutonic and volcanic rocks based on thermodynamics and kinetic considerations; *Geochim. Cosmochim. Acta* **48** 1523–1534.

Pal T 2011 Petrology and geochemistry of the Andaman ophiolite: Melt–rock interaction in a suprasubduction-zone setting; *J. Geol. Soc. London* **168** 1031–1045.

Pal T and Bhattacharya A 2010 Greenschist-facies, subophiolitic metamorphic rocks of Andaman Islands, Burma–Java subduction complex; *J. Asian Earth Sci.* **39** 804–814.

Pal T, Chakraborty P P, Duttagupta T and Singh D 2003 Geodynamic evolution of outer arc–forearc belt in the Andaman Islands, the central part of the Burma–Java subduction complex; *Geol. Mag.* **140** 289–307.

Pandey J, Agarwal R P, Dave A, Maithani A, Trivedi K B, Srivastava A K and Singh D N 1992 Geology of Andaman; *Bull. ONGC* **2(2)** 19–103.

Pedersen R B, Searle M P, Carter A and Bandopadhyay P C 2010 U–Pb zircon age of Andaman ophiolite: Implications for the beginning of subduction beneath the Andaman–Sumatra subduction arc; *J. Geol. Soc. London* **167** 1105–1112.

Rahman M J and Suzuki S 2007 Geochemistry of sandstones from the Miocene Surma Group, Bengal Basin, Bangladesh: Implications for provenance, tectonic setting and weathering; *Geochem. J.* **41** 415–428.

Rajashekhar C and Reddy P P 2003 Quaternary stratigraphy of the Andaman-Nicobar Islands, Bay of Bengal; *J. Geol. Soc. India* **62** 485–493.

Raju K A K 2005 Three-phase tectonic evolution of the Andaman backarc basin; *Curr. Sci.* **89(11)** 1932–1936.

Rashid S A 2002 Geochemical characteristics of Mesoproterozoic clastic sedimentary rocks from Chakrata Formation, Lesser Himalaya: Implications for crustal evolution and weathering history in the Himalaya; *J. Asian Earth Sci.* **21** 283–293.

Raza M, Casshyap S M and Khan A 2002 Geochemistry of Mesoproterozoic Lower Vindhyan shales from Chattaurgarh, southeastern Rajasthan and its bearing on source rock composition, paleoweathering conditions and tectono-sedimentary environments; *J. Geol. Soc. India* **60** 505–518.

Roser B P and Korsch R J 1986 Determination of tectonic setting of sandstone–mudstone suites using SiO_2 content and K_2O/Na_2O ratio; *J. Geol.* **94** 635–650.

Roy D K, Acharyya S K, Ray K K, Lahri T C and Sen M K 1988 Nature of occurrence, age and depositional environment of the oceanic pelagic sediments associated with ophiolite assemblage, South Andaman Island, India; *Indian Minerals* **42** 31–65.

Roy T K 1983 Geology and hydrocarbon prospects of Andaman–Nicobar; In: Petroliferous Basins of India (eds) L L Bhandari *et al.*, *Petroleum Asia J.*, pp. 3–50.

Sarma D S, Jafri S H, Fletcher I R and McNaughton N J 2010 Constraints on the tectonic setting of the Andaman ophiolites, Bay of Bengal, India, from SHRIMP U–Pb zircon geochronology of plagiogranite; *J. Geol.* **118** 691–697.

Sharma V and Srinivasan M S 2007 Geology of Andaman–Nicobar: The Neogene; Capital Publishing Company, New Delhi, Kolkata, Bangalore.

Taylor S R and McLennan S M 1985 The Continental Crust: Its composition and evolution; Blackwell Publishing Company, USA, UK, Australia, 311p.

Tucker M E 2001 Sedimentary petrology: An introduction to the origin of sedimentary rocks; 3rd edn, Blackwell Publishing Company, USA, UK, Australia, India, pp. 1–251.

Turekian K K and Wedepohl K H 1961 Distribution of the elements in some major units of the earth's crust; *Geol. Soc. Am. Bull.* **72** 175–192.

Verma S P and Armstrong-Altrin J S 2013 New multidimensional diagrams for tectonic discrimination of siliciclastic sediments and their application to Precambrian basins.

Vohra C P, Haldar D and Gosh Roy A K 1989 The Andaman–Nicobar ophiolite complex and associated mineral resources-current appraisal; In: Phanerozoic ophiolite of India (ed.) Ghosh N C, Sumana Publisher, Patna, India, pp. 281–315.

Wrafter J P and Graham J R 1989 Short Paper: Ophiolitic detritus in the Ordovician sediments of South Mayo, Ireland; *J. Geol. Soc. London* **146** 213–215.

Wronkiewicz D J and Condie K C 1987 Geochemistry of Archean shales from the Witwatersrand Supergroup, South Africa: Source-area weathering and provenance; *Geochim. Cosmochim. Acta* **51** 2401–2416.

Young G M and Nesbitt H W 1998 Process controlling the distribution of Ti and Al in weathering profiles, siliciclastic sediments and sedimentary rocks; *J. Sedim. Res.* **68** 448–455.

MS received 16 September 2014; accepted 31 January 2015